Electronic Supplementary Information

An integrated carbonized wood-based gas-diffusion electrode for high-current-density CO electrosynthesis in the flow cells

Huanhuan Tao,[a,b,c,§] Huaiyu Chang,[a,b,c,d,§] Fang Wang,[a,b,c] Zhengguo Zhang,[a,b,d] and Shixiong Min[a,b,c*]

[a] *School of Chemistry and Chemical Engineering, North Minzu University, Yinchuan, 750021, P. R. China. E-mail: sxmin@nun.edu.cn*

[b] *Ningxia Key Laboratory of Solar Chemical Conversion Technology, North Minzu University, Yinchuan 750021, P. R. China.*

[c] *Key Laboratory of Chemical Engineering and Technology, State Ethnic Affairs Commission, North Minzu University, Yinchuan, 750021, P. R. China.*

[d] *Institute of Sustainability for Chemicals, Energy and Environment (ISCE^2), Agency for Science, Technology and Research (A*STAR); 1 Pesek Road, Jurong Island, 627833, Singapore.*

[§] These two authors contributed equally to this work.

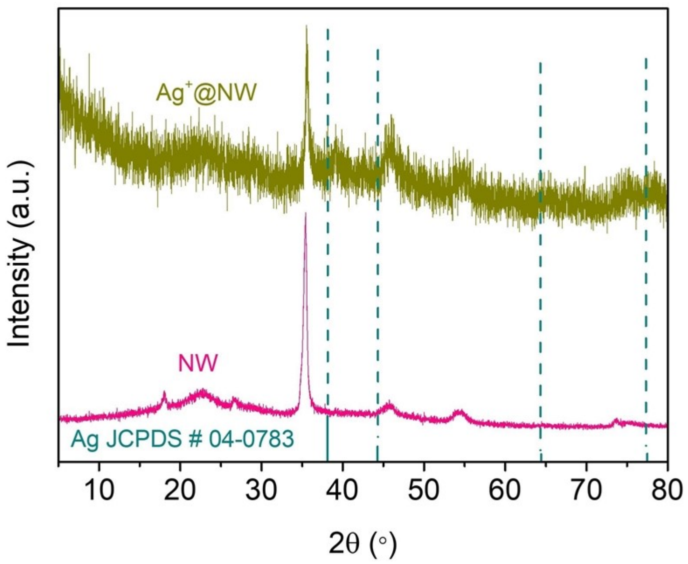

Fig. S1 XRD patterns of NW and Ag^+@NW.

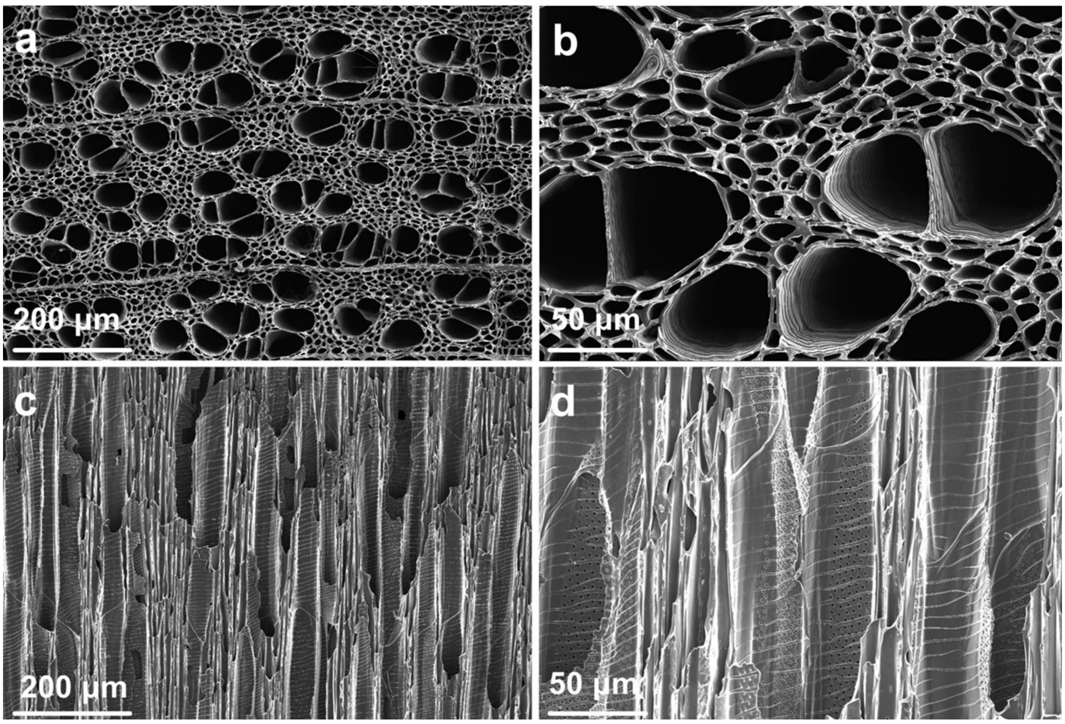

Fig. S2 (a, b) Top-view and (c, d) side-view SEM images of CW electrode.

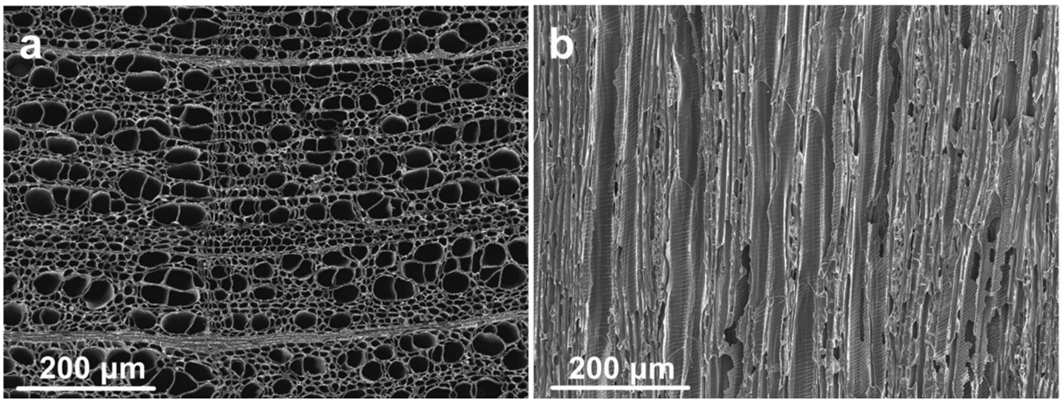

Fig. S3 (a) Top-view and (b) side-view SEM images of Ag@CW electrode.

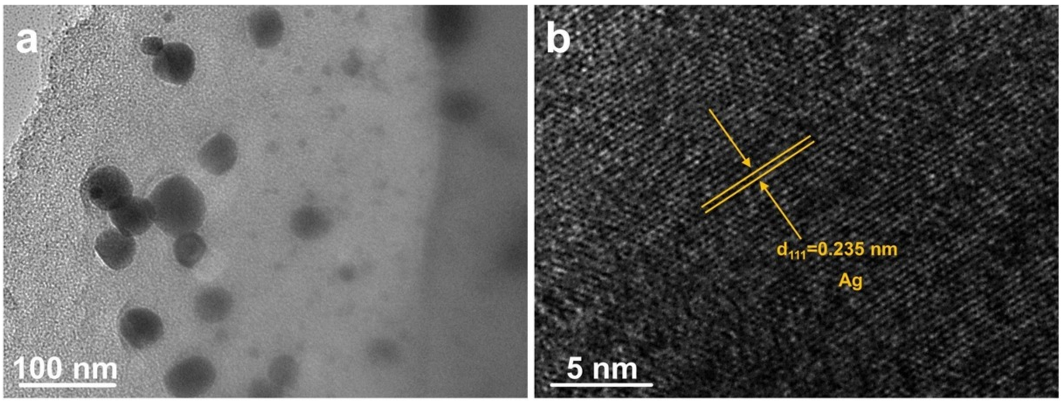

Fig. S4 (a) TEM and (b) HRTEM images of Ag@CW electrode.

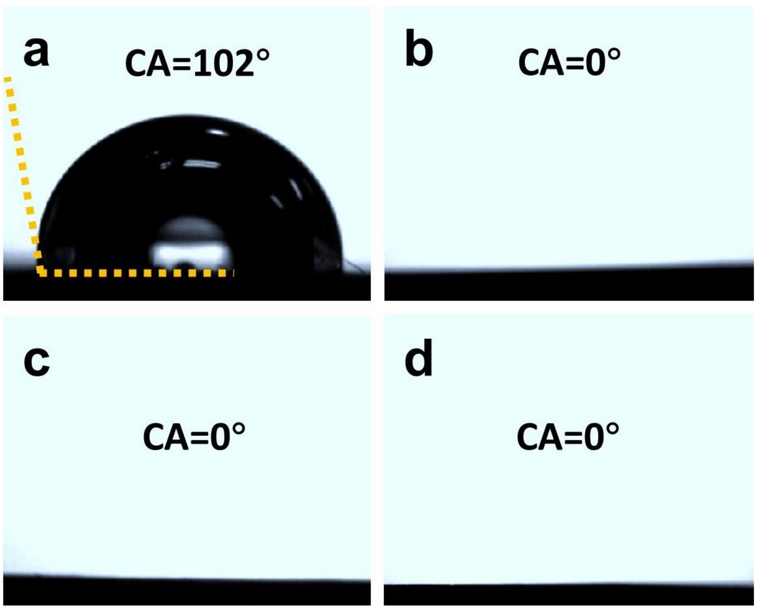

Fig. S5 The electrolyte contacts angels for (a) Ag@CW, (b) Ag@CW-E, (c) Ag@CW-EO, and (d) Ag@CW-ER electrodes.

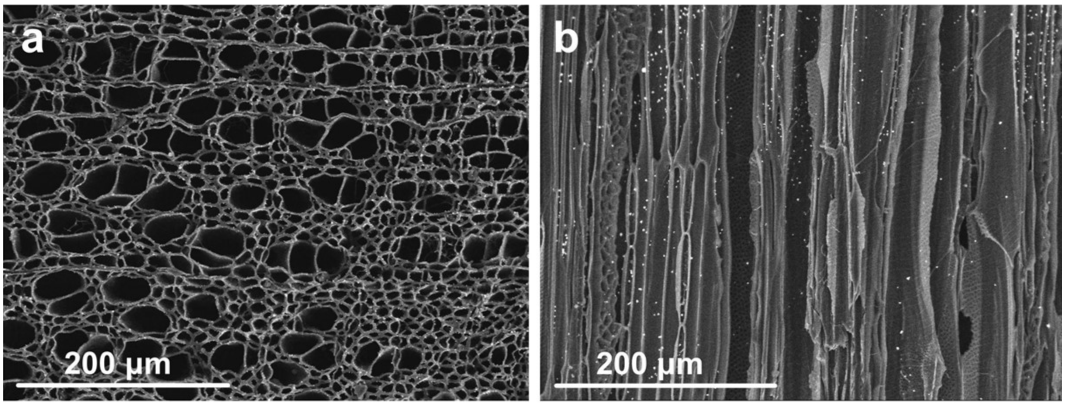

Fig. S6 (a) Top-view and (b) side-view SEM images of Ag@CW-E electrode.

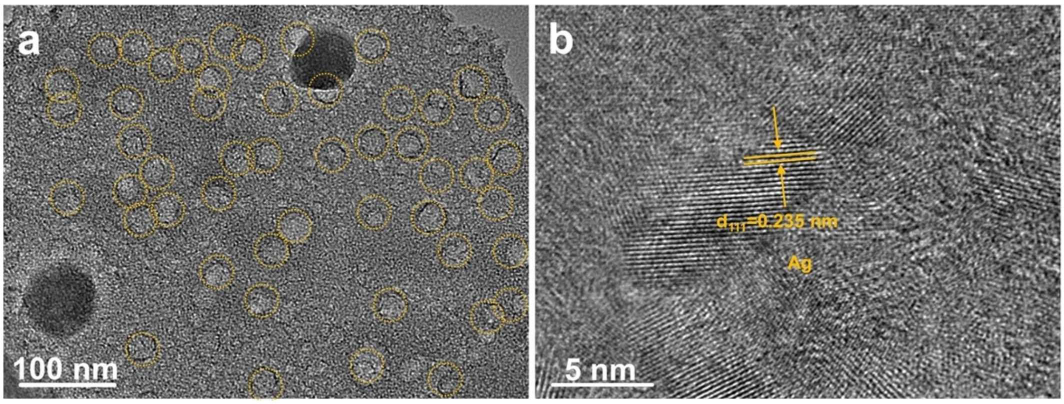

Fig. S7 (a) TEM and (b) HRTEM images of Ag@CW-E electrode.

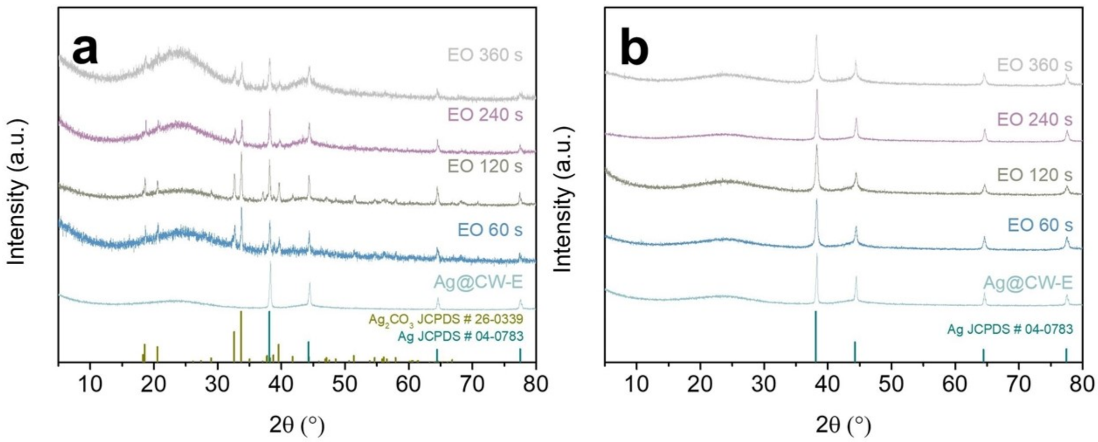

Fig. S8 (a) XRD patterns of Ag@CW-E electrodes prepared at different electrochemical oxidation times and (b) the corresponding Ag@CW-ER obtained after electrochemical reduction at -0.5 V vs. Ag/AgCl for 600 s.

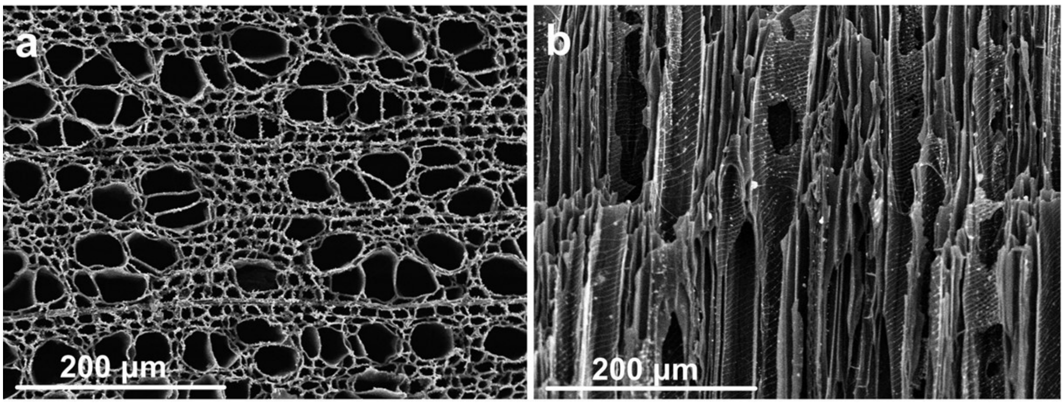

Fig. S9 (a) Top-view and (b) side-view SEM images of Ag@CW-EO electrode.

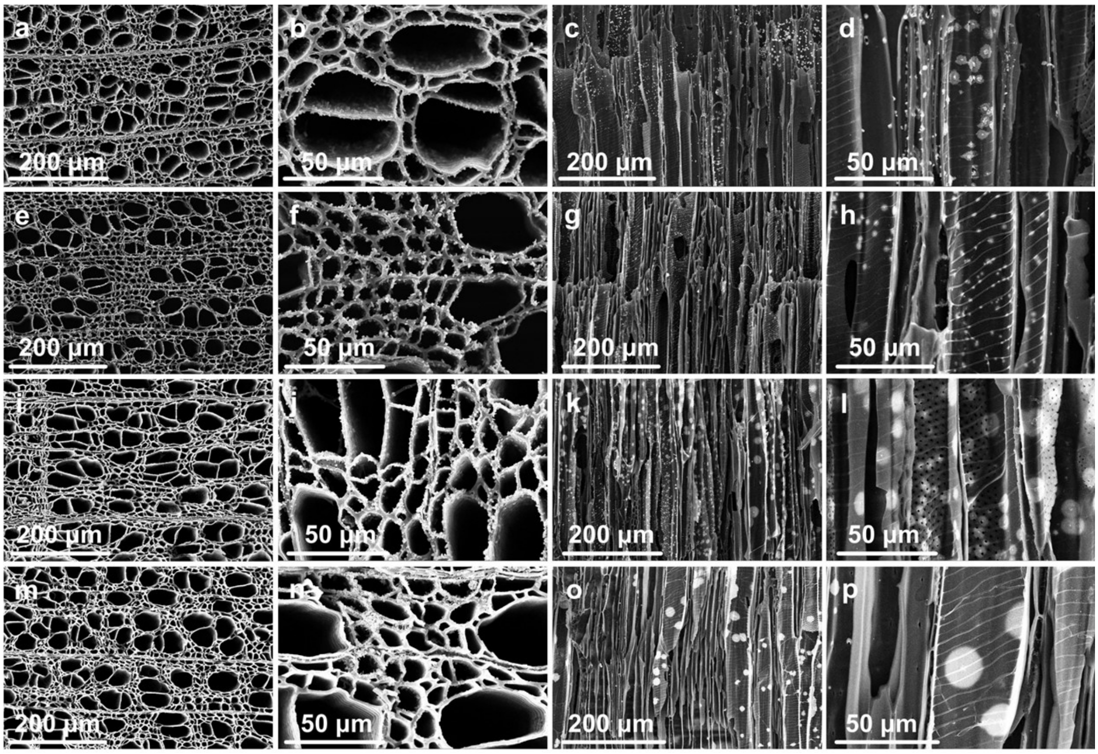

Fig. S10 Top-view and side-view SEM images of Ag@CW-EO electrodes prepared at electrochemical oxidation time of (a-d) 60 s, (e-h) 120 s, (i-l) 240 s, and (m-p) 360 s.

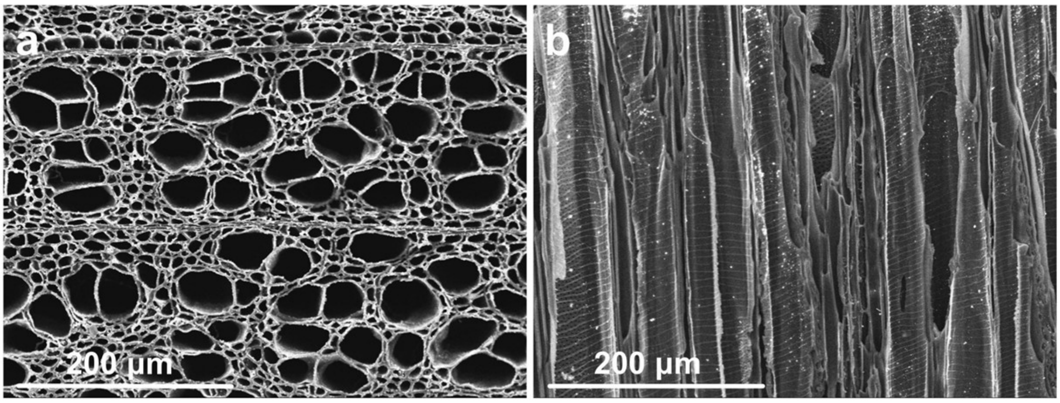

Fig. S11 (a) Top-view and (b) side-view SEM images of Ag@CW-ER electrode.

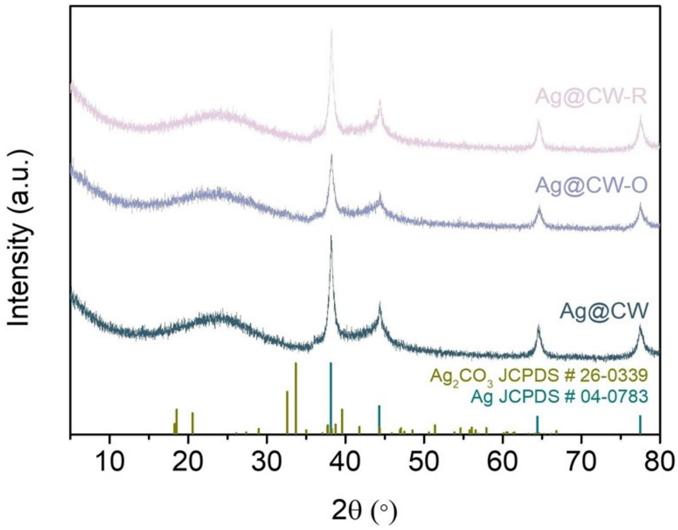

Fig. S12 XRD patterns of Ag@CW, Ag@CW-O, and Ag@CW-R electrodes.

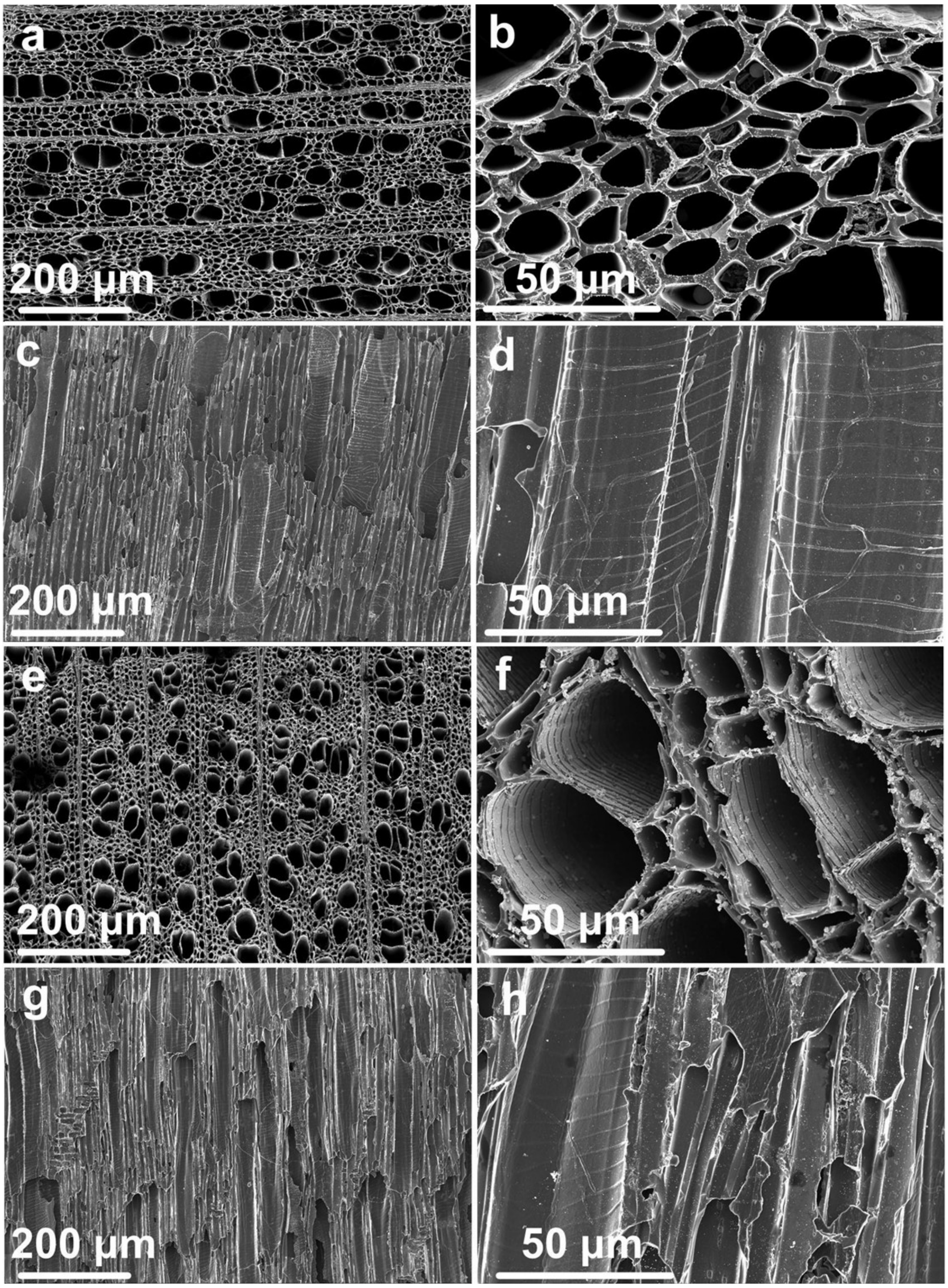

Fig. S13 (a, b) Top-view and (c, d) side-view SEM images of Ag@CW-O electrode. (e, f) Top-view and (g, h) side-view SEM images of Ag@CW-R electrode.

Table S1 Textural parameters of CW, Ag@CW, Ag@CW-E, Ag@CW-EO, and Ag@CW-ER electrodes.

Electrodes	S_{BET} ($m^2\ g^{-1}$)	Pore volume ($cm^3\ g^{-1}$)	Pore size (nm)
CW	103.9	0.06	2.39
Ag@CW	26.1	0.02	2.65
Ag@CW-E	587.6	0.32	2.15
Ag@CW-EO	461.3	0.25	2.18
Ag@CW-ER	447.7	0.24	2.19

Table S2 Ag contents in the electrodes determined by ICP-OES analysis.

Electrodes	Ag@CW	Ag@CW-E	Ag@CW-EO	Ag@CW-ER
Ag(wt%)	2.46	3.05	1.87	2.28

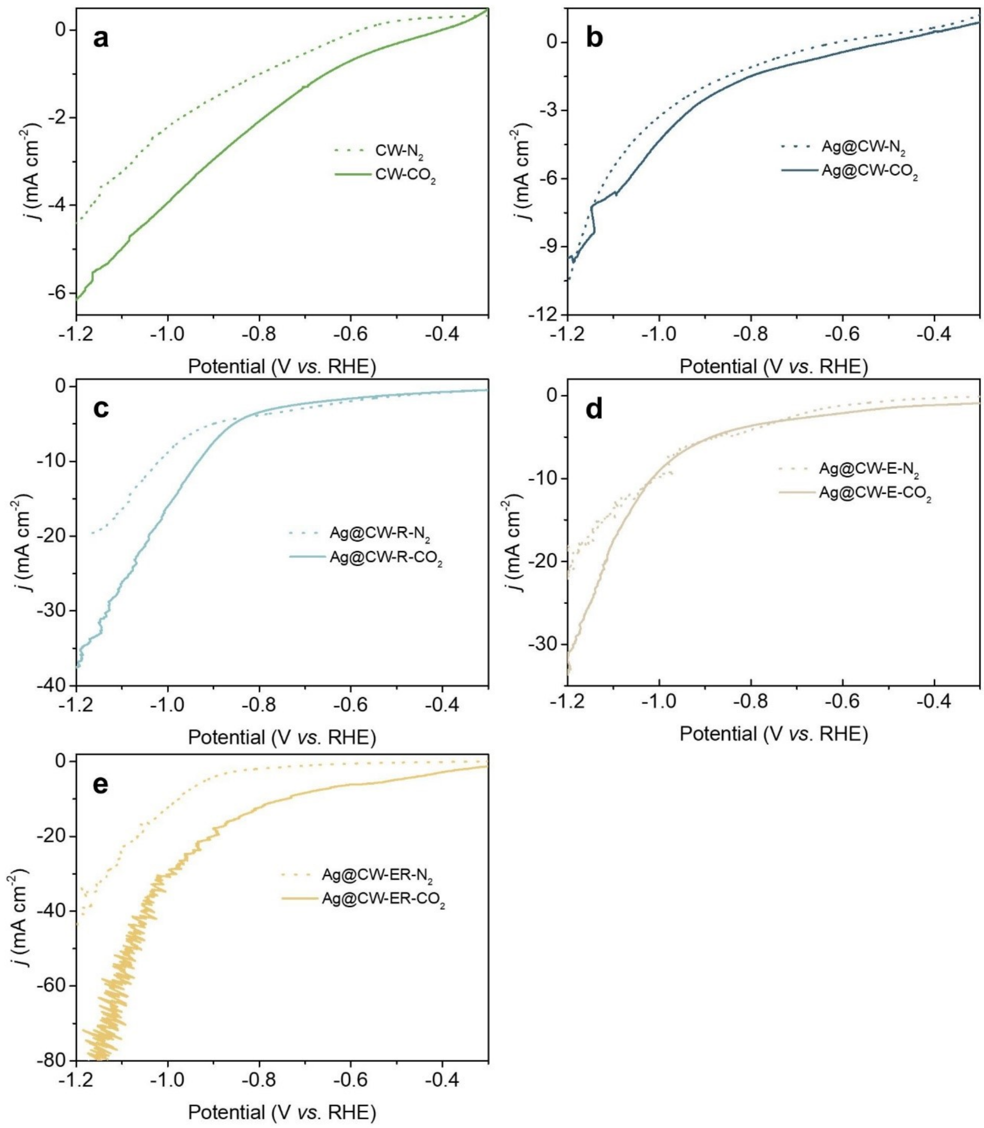

Fig. S14 LSV curves of various electrodes in the N_2 and CO_2-saturated 0.1 M $KHCO_3$

aqueous solution with a scan rate of 0.5 mV s^{-1}.

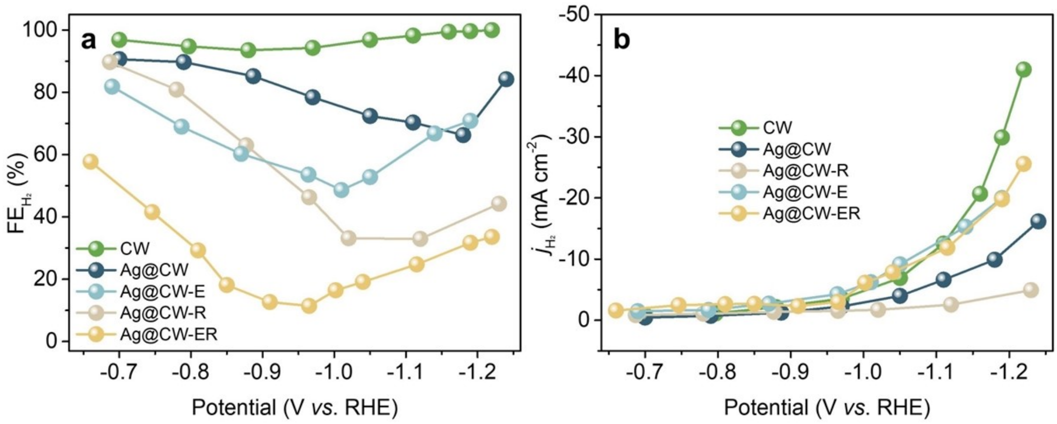

Fig. S15 (a) FEs and (b) partial current densities for H_2 production for CW, Ag@CW, Ag@CW-E, Ag@CW-R and Ag@CW-ER electrodes at various applied potentials.

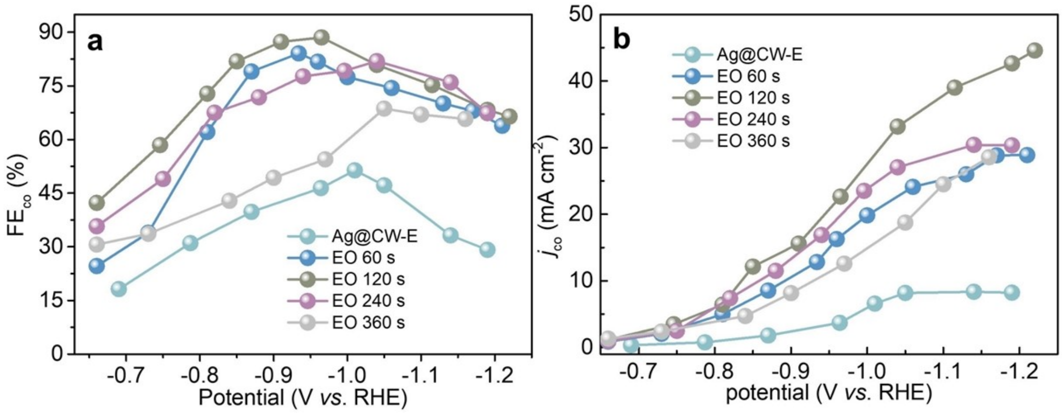

Fig. S16 (a) FE and (b) partial current density for CO production over Ag@CW-ER electrodes derived from Ag@CW-EO prepared at different electrochemical oxidation times.

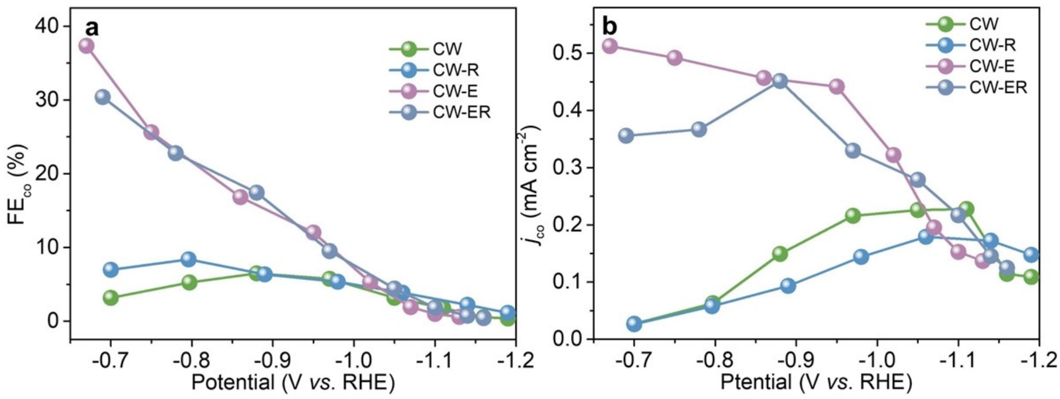

Fig. S17 (a) FE and (b) partial current density for CO production over CW, CW-R, CW-E, and CW-ER electrodes as a function of applied potential.

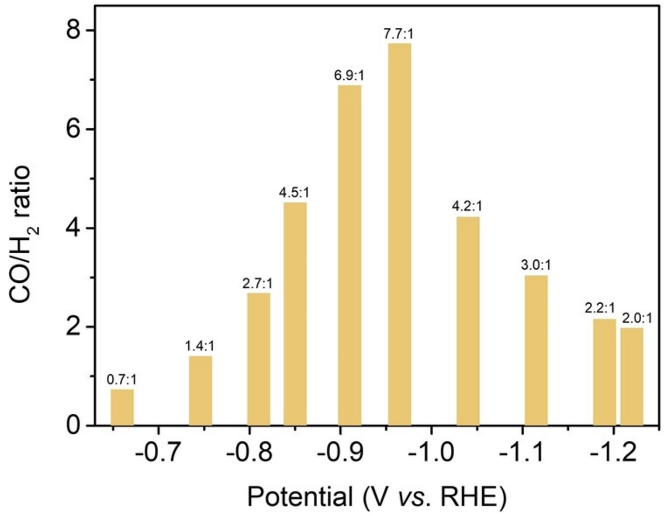

Fig. S18 Dependence of CO/H_2 ratio over Ag@CW-ER electrode as a function of applied potential.

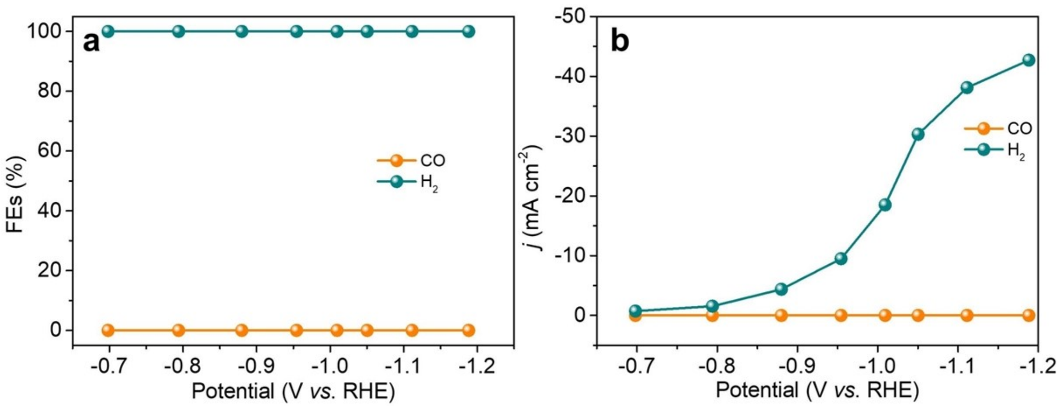

Fig. S19 (a) FEs and (b) current densities for CO and H_2 production over Ag@CW-ER electrode in a N_2-saturated 0.1 M $KHCO_3$ solution at various applied potentials.

Table S3 Comparison of CO_2RR performance of Ag@CW-ER with recently reported Ag-based catalysts.

Catalysts	Electrolyte ($KHCO_3$)	*E* (V vs RHE)	FE_{CO} (%)	j_{CO} (mA cm^{-2})	Ref.
5 nm Ag/C	0.5 M	-0.75	84.4	~4	[1]
Ag_2-G	0.5 M	-0.7	93.4	11.87	[2]
Ag-Nano-Pre100	0.1 M	-1.2	~70	~15	[3]
Ag/CNT-COOH	0.1 M	-1.1	83	~18	[4]
NP-Ag	0.1 M	-0.9	93	~7	[5]
Ag_1-MnO_2	0.5 M	-0.85	95.7	~2.5	[6]
Ag NWs/NC700	0.1 M	-1.15	81	~22.8	[7]
CB/Ag NWs	0.5 M	-1.16	~89	~4.2	[8]
Ag-2-C16	0.5 M	-0.8	97	1.21	[9]
Oxide-derived Ag	0.1 M	-0.6	80	0.3	[10]
Tri-Ag-NPs	0.1 M	-0.856	96.8	1.25	[11]
D-25 Ag NWs	0.1 M	-0.956	99.3	2.25	[12]
C-Ag	0.5 M	-0.95	62.7	4	[13]
Cu/Ag(S)	0.1 M	-1.0	93.0	2.9	[14]
Ag-P@HCS	0.5 M	-0.8	70.1	~5	[15]
Ag-NDs/Zn-NLs	0.1 M	-1.0	85.2	8.12	[16]
$In(OH)_3$-Ag/C	0.1 M	-0.7	93	~2.5	[17]
Cr_2O_3@Ag	0.5 M	-0.8	99.6	19.0	[18]
2 nm-Ag NCs	0.1 M	-0.76	93.8	0.88	[19]
Ag_2S-Au	0.5 M	-0.8	94.5	9.17	[20]
Ag@CW-ER	**0.1 M**	**-0.97** **-1.22**	**88.55** **66.5**	**22.64** **44.6**	**This work**

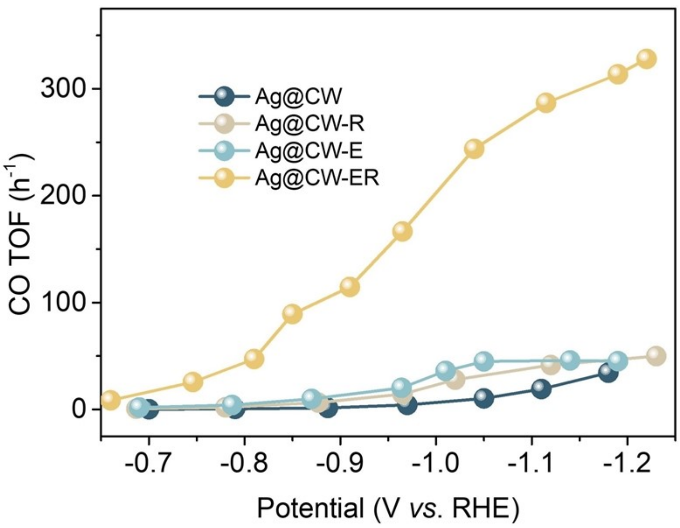

Fig. S20 TOFs of CO production over Ag@CW, Ag@CW-R, Ag@CW-E, and

Ag@CW-ER electrodes at different applied potentials.

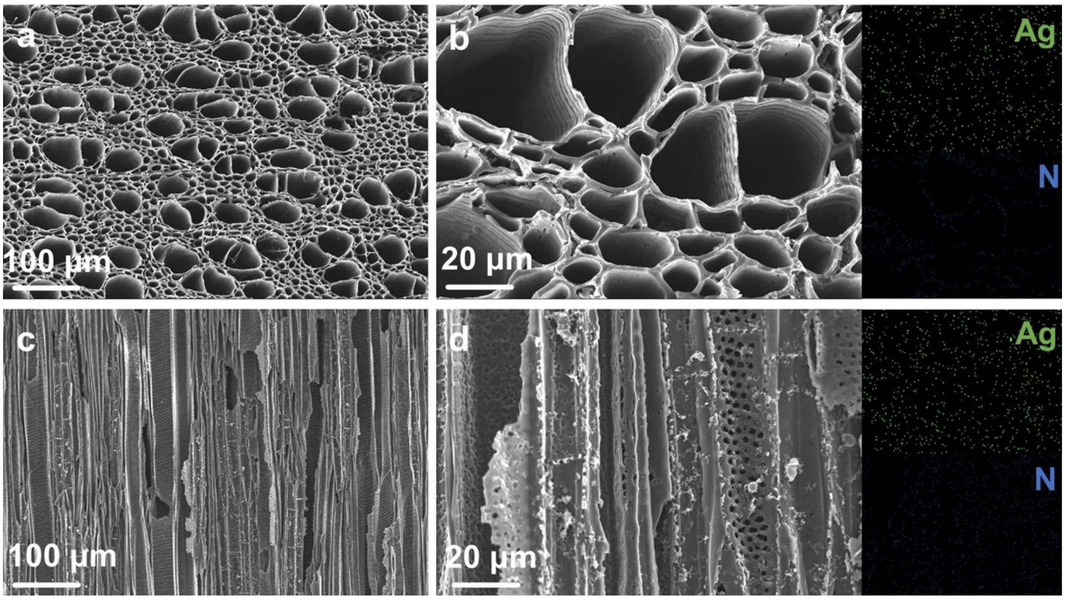

Fig. S21 (a and b) Top-view and (c and d) side-view SEM images of Ag@CW-ER electrode after CO_2RR stability test and the corresponding EDX element maps.

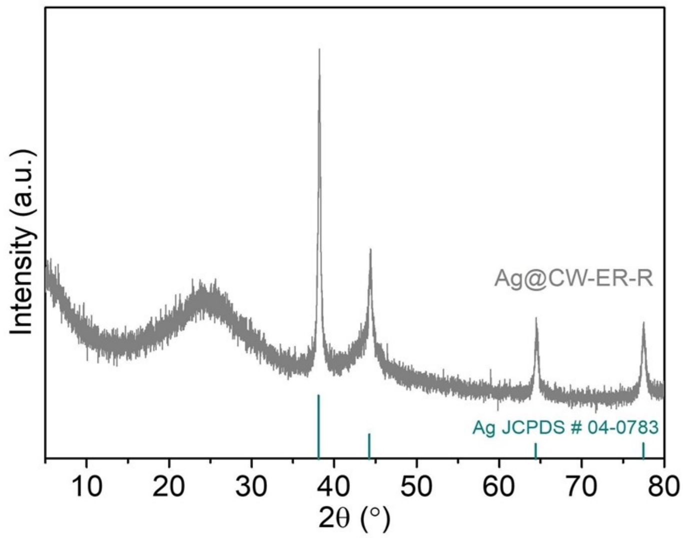

Fig. S22 XRD pattern of Ag@CW-ER electrode after CO_2RR stability test.

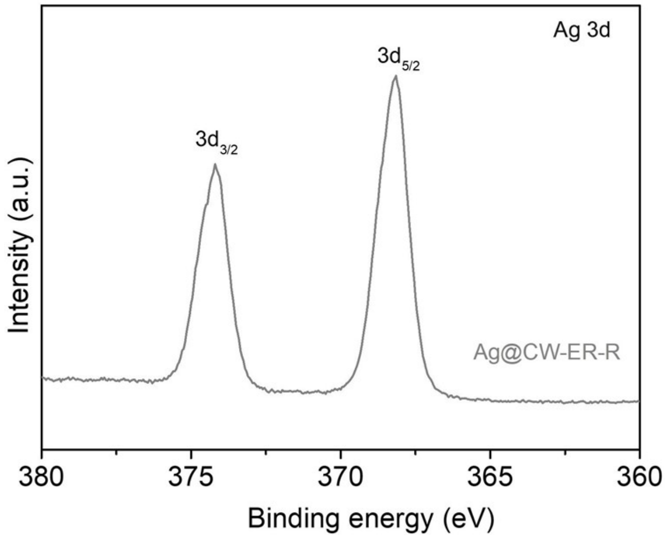

Fig. S23 Ag 3d XPS spectrum of Ag@CW-ER electrode after CO_2RR stability test.

References

1. C. Kim, Jeon, H. S. Jeon; T. Eom, M. S. Jee, H. Kim, C. M. Friend, B. K. Min and Y. J. Hwang, *J. Am. Chem. Soc.*, 2015, **137**, 13844-13850.
2. Y. F. Li, C. Chen, R. Cao, Z. W. Pan, H. He and K. B. Zhou, *Appl. Catal., B*, 2020, **268**, 118747.
3. Z. J. Wang, T. F. Li, Q. H. Wang, A. X. Guan, N. Cao, A. M. Al-Enizi, L. J. Zhang, L. P. Qian and G. F. Zheng, *J. Power Sources*, 2020**, 476**, 228705.
4. J. L. Sun, J. Xu, H. Jiang, X. S. Zhang and D. F. Niu*,* *ChemElectroChem*, 2020, **7**, 1869-1876.
5. T. T. Fan, Q. L. Wu, Z. Yang, Y. P. Song, J. G. Zhang, P. P. Huang, Z. Chen, Y. Y. Dong, W. P. Fang and X. D. Yi, *ChemSusChem*, 2020, **13**, 2677-2683.
6. N. Q. Zhang, X. X. Zhang, L. Tao, P. Jiang, C. L. Ye, R. Lin, Z. W. Huang, A. Li, D. W. Pang, H. Yan, Y. Wang, P. Xu, S. F. An, Q. H. Zhang, L. C. Liu, S. X. Du, S. D. Han, D. S. Wang and Y. D. Li, *Angew. Chem. Int. Ed.*, 2020, **60**, 6170-6176.
7. H. P. Yang, H. W. Zhang, Y. Wu, L. D. Fan, X. Y. Chai, Q. L. Zhang, J. H. Liu and C. X. He, *ChemSusChem*, 2018, **11**, 3905–3910.

8. X. Z. Wang, S. B. Liu, Q. X. Liu and J. L. Luo, *Electrochem. Commun*. 2019, **107,** 106531.
9. A. K. Buckley, T. Cheng, G. M. Su, J. Garrison, S. W. Utan, C. H. Zhu, F. D. Toste, W. A. Goddard and F. M. Toma, *ACS Catal*., 2021, **11**, 9034–9042.
10. M. Ma, B. J. Trześniewski, J. Xie and W. A. Smith, *Angew. Chem. Int. Ed.,* 2016, **55,** 9748-9752.
11. S. B. Liu, H. B. Tao, L. Zeng, Q. Liu, Z. H. Xu, Q. X. Liu and J. L. Luo, *J. Am. Chem. Soc*., 2017, **139**, 2160-2163.
12. S. B. Liu, X. Z. Wang, H. Tao, T. F. Li, Q. Liu, Z. H. Xu, X. Z. Fu and J. L. Luo, *Nano Energy,* 2018, **45**, 456-462.
13. M. Yang, J. Z. Zhang, Y. Y. Cao, M. F. Wu, K. Qian, Z. H. Zhang, H. Y. Liu, J. G. Wang, W. Chen and W. X. Huang, *ChemCatChem*, 2018, **10**, 5128-5134.
14. Z. Ma, T. Wan, D. Zhang, J. A. Yuwono, C. Tsounis, J. Jiang, Y.-H. Chou, X. Lu, P. V. Kumar, Y. H. Ng, D. Chu, C. Y. Toe, Z. Han and R. Amal, *ACS Nano*, 2023, **17**, 2387-2398.
15. K. Li, Y. Kuwahara and H. Yamashita, *Appl. Catal. B Environ.*, 2023, **331**, 122713.
16. S. Yang, M. Jiang, M. Wang, L. Wang, X. Song, Y. Wang, Z. Tie and Z. Jin, *Nano Res.*, 2023, **16**, 8910-8918.
17. L. Fu, Z. Qu, L. Zhou and Y. Ding, *Appl. Catal. B Environ.*, 2023, **339**, 123170.
18. H. Q. Fu, J. Liu, N. M. Bedford, Y. Wang, J. W. Sun, Y. Zou, M. Dong, J. Wright, H. Diao, P. Liu, H. G. Yang and H. Zhao, *Adv. Mater.,* 2022, **34**, 2202854.
19. H.-C. Mi, C. Yi, M.-R. Gao, M. Yu, S. Liu and J.-L. Luo, *ACS Appl. Mater. Interfaces,* 2022, **14**, 43257-43264.
20. Q. S. Chen, P. L. Cui, J. Yang, D. Chen, H. Liu, H. Feng, P. Tsiakaras and P. K.

Shen, *J. Colloid Inter. Sci.*, 2022, **623**, 1172-1180.